ASIAN JOURNAL OF MATHEMATICS AND APPLICATIONS
Volume 2016, Article ID ama0284, 23 pages
ISSN 2307-7743
http://scienceasia.asia

# SORET- DUFOUR AND STRESS WORK EFFECTS ON HYDROMAGNETIC FREE CONVECTION OF A CHEMICALLY REACTIVE STAGNATION SLIP-FLOW AND HEAT TRANSFER TOWARDS A STRETCHING VERTICAL SURFACE WITH HEAT GENERATION AND VARIABLE THERMAL CONDUCTIVITY

ADETUNJI ADENIYAN

**Abstract:** Investigation was carried out on steady two-dimensional free convective flow and heat transfer of a boundary layer hydromagnetic flow over a stretching porous vertical sheet embedded in an expanse of an incompressible, and electrically conducting fluid awash of uniform transverse magnetic field in the presence of combined influences of stress work, exponentially decaying heat generation, Soret and Dufour alongside the suction/ injection. It was assumed that the thermal conductivity of the fluid was a linear function of temperature. Using appropriate similarity variables, the governing non-linear PDEs are transformed into a set of ODEs together with the considered BCs, which were solved numerically by shooting iteration method coupled with the fourth order classical Runge-Kutta integration scheme through a reliable computation software package. A comparison with previously published results on the similar special cases was accessed, and the results were found to be in perfect agreement. The effects of Prandtl number, Eckert number, buoyancy force, Lorentz force, the thermal heat generation, thermal-diffusion, diffusion-thermo, velocity ratio and mass blowing/fluid suction on the fluid behavior were delineated in physical terms. Finally, numerical values of pertinent physical quantities, such as the skin-friction coefficient, the local Nusselt and Sherwood numbers were sorted out and presented in tabular form while those of the dimensionless fluid velocity, temperature and concentration were addressed and discussed by graphs. Our findings reveal that all the basic emerging flow parameters significantly influence the heat and mass characteristics of the flow.

## 1. Introduction

The behaviors of viscous fluid under the boundary-layer flow due to a moving sheet in cognizance with the condition of natural convection, for a quiescent or a moving ambient stream, are incredibly dominant in many technological and industrial processes involving cooling of nuclear reactors, electronics and chemical devices, processing equipments, drying, electricity generating plant cooling towers and many others. In a stagnation point boundary layer flow about a stretching sheet, the distribution of solutes capable of undergoing chemical reactions play a significant role as duly practiced in the metallurgical production of steel and copper wire, and plates annealing and tinning. Specifically, some of these processes which involve heat and mass transfer are subject to surface temperature control in the manufacturing industries for topnotch quality of penultimate products with

Key words and phrases: Hydromagnetics, variable thermal conductivity, slip velocity, chemical reaction, diffusion-thermo, thermal-diffusion, stress work, permeable sheet.

desired characteristics. Most often it is necessary to introduce magnetic field into the flow regime of boundary layer flow of an electrically conducting, viscous fluid as this may serve as a means of reducing the speed which consequently impedes the influence of separation or postpone transition. Prandtl, after his proposed boundary layer theory in 1904 (see Anderson, 2005), demonstrated that the boundary layer approximation facilitated a means for flow separation control. His slotted cylinder experiment clearly indicates that suction stems down the boundary layer thickness and reduces the wall drag force. The classical boundary layer approximation was pioneered by Hiemenz (1911) to solve exactly steady two-dimensional momentum equation for a stagnation point flow and obtained similarity results. Crane (1970), studied steady two-dimensional boundary-layer flow induced by linear stretching of the sheet using similarity analysis. Since then, several studies on heat and mass transfer incorporating some other thermophysical effects into the boundary layer flow for a stagnation point flow have appeared in the literature (Makinde and Charles, 2010; Yian et al., 2011; Mahapatra and Nandi, 2013; Olanrewaju and Adesanya, 2011; Wong et al., 2013; Adeniyan and Adigun, 2013; Oahimire and Olajuwon, 2013; Chen, 2014; Arthur and Seini, 2014), among others. The behavior of Magnetohydrodynamics (MHD) boundary layer flow over a stretching rigid surface abounds in an electrically conducting fluid, exposed to a transverse magnetic field is being utilized in many modern technological processes such as in the field of metallurgy exemplified by MHD stirring of molten metal and magnetic levitation casting, and also petrochemical and geothermal applications for enhanced crude oil and geothermal energy extractions, and several others. Heat and mass transfer problems over a permeable stretching surface in an electrically conducting fluid, permeated by a transverse magnetic field have been presented by Ibrahim and Makinde (2010, 2011), Makinde and Charles (2010), Usman and Uwanta (2013), Makinde et al. (2013), Akbar et al. (2014), a few among others. Thermal conductivity in a fluid is that property in virtue of which it is able to offer penetration of thermal convection. The coefficient of thermal conductivity is not a constant, but in general depends on fluid temperature. For example, the thermal conductivity of liquid metals varies with temperature in an approximately linear manner in the range from $0^0$ F to $400^0$ F ( Rangi and Ahmad, 2012; Hayat et al., 2014). However, Moitsheki and Makinde (2013) utilized the power law temperature dependence, whereas Mahanta (2013) employed linear inverse function temperature dependence for thermal conductivity in their respective models. In several problems of heat and mass transfer convective flows concerning chemical reaction of species concentration as exemplified in petro-chemical engineering and industrial processes for drying, chemical particulate deposition on surfaces, cooling towers of thermal power plant, nuclear waste repositories, packed bed catalytic reactors, fluidized

reactors, thermonuclear energy confinement, astrophysics and space science, etc. Keeping this in view, a pretty number of researchers in the recent past has shown renewed interest for intensive investigations of effect of chemical reaction mechanism on boundary layer-flow for momentum, energy and mass transfer transport models. Ibrahim and Makinde (2010, 2011) investigated the effects of chemical reaction on MHD boundary layer flow over a vertically moving sheet with heat and mass transfer characteristics. Stress wok in a Newtonian fluid is an intrinsic property which represents the work done by a unit mass of the fluid against the external force acting on a unit surface area of the fluid. In many chemical engineering and industrial processes, chemical reactions feature between a working fluid and a foreign mass which is often associated with stress work. However, sparse work has been done which considered this physical influence on the behavior of Newtonian boundary layer flow in the recent past. Khan et al. (2003) studied viscoelastic MHD boundary layer flow, heat and mass transfer past a stretching permeable sheet with dissipation energy and stress work. Joshi and Gebhart (1981) analyzed the effect of the pressure stress work and viscous dissipation in some natural convection flow the case for isothermal, uniform flux and plumes. Little attention has been paid to the studies incorporating the influence of surface velocity slip into the context of boundary layer flow problems. In the so-called no-slip solid surface boundary conditions, the action of viscosity prevents a discontinuity in the velocity between the surface and the fluid. However, the concept which establishes differences in these physical quantities at the solid surface gives rise to slip conditions. Violation in the no-slip conditions manifests when the molecular mean-free path becomes comparable with the distances involved. In practice, this surface boundary condition mechanism is exhibited for processes which involve polishing of internal cavities and artificial heart valves in bioengineering and medicine. The combined influence of magnetic field and permeable walls slip velocity on the steady flow of a hydromagnetic fluid in a channel was reported by Makinde and Osalusi (2006). More recently, heat and mass transfer boundary layer slip flow of hydromagnetic fluid past a chemically reactive plate awash of transverse magnetic field was reported by Singh and Makinde (2013). Their model presumed that the surface reacted with the fluid which produced inert species and the species mass flux varied directly as the concentration at the plate surface. A few, amongst other recent investigators who incorporated into their studies the effects of slips include (Aman and Ishak, 2011; Bhattacharyya and Mukhopadhyay, 2013; Eegunjobi and Makinde, 2012; Makinde 2012; Ibrahim and Reddy, 2013; Chen, 2014; Adeniyan and Adigun, 2014). The practical importance of heat source or heat generation may arise from a variety of causes such as radioactivity, dissociating fluids, fluid undergoing exothermic or endothermic chemical reactions, release of latent heat due

to water vapor condensation the occurrence of which is observable when rain is about to fall, etc., the reverse cause of which may constitute heat sink or absorption. The heat generation or absorption in its effects on thermal convection may become significant when there occurs appreciable high temperature differences between two surfaces as in the case for space vehicles and the ambient fluids. Quite a number of studies on boundary layer flow alongside the heat and mass transfer incorporating the effects of internal heat generation or absorption has appeared in the literature ( Seddeek, 2004; Oahimire and Olajuwon, 2013; Shrama and Sing, 2010; Abel and Mahesha, 2008; Olanrewaju, 2012; Makinde and Olanrewaju, 2012). In several problems of heat and mass transfer convective flows concerning chemical reaction of species concentration as exemplified in petro-chemical engineering and industrial processes for drying, chemical particulate deposition on surfaces, cooling towers of thermal power plant, nuclear waste repositories, packed packed bed catalytic reactors, fluidized reactors, thermonuclear energy confinement, astrophysics and space science, etc. Keeping this in view, a pretty number of researchers in the recent past has shown renewed interest for intensive investigations of effect of chemical reaction mechanism on boundary layer-flow for momentum, energy and mass transfer transport models The combined influence of magnetic field and permeable walls slip velocity on the steady flow of a hydromagnetic fluid in a channel was reported by Makinde and Osalusi (2006). More recently, heat and mass transfer boundary layer slip flow of hydromagnetic fluid past a chemically reactive plate awash of transverse magnetic field was reported by Singh and Makinde (2013). Their model presumed that the surface reacted with the fluid which produced inert species and the species mass flux varied directly as the concentration at the plate surface. The diffusion-thermo ( Dufour) and thermal diffusion (Soret) effects have considerable effects on the boundary layer flow of a viscous fluid in the neighborhood of a moving solid surface awash of saturated porous medium and their inclusion in phenomenal fluid flow becomes relevant and non-ignorable. The thermal energy flux induced by a solute or concentration gradient is referred to as Dufour effect while the mass or concentration flux originating from temperature gradient is termed Soeret effect. Such flows have attracted a number of scholars because of their usefulness in practical engineering situations such as, in the field of agro-engineering and petro-chemical technology for management of underground water and crude oil resources, and also industrial process requiring isotope separation etc. In view of this, Adrain (2010) presented his study on heat and mass transfer by free convection for a stagnation point flow in the presence of Soret and Dufour effects, Bazid et al.(2012) studied numerically the stagnation flow towards a uniformly heated vertical plate with the variable thermal conductivity, Dufour and Soret effects while Olanrewaju and Gbadeyan (2011) examined

the effects of Soret, Dufour, chemical reaction, thermal radiation and heat generation/absorption on mixed convection stagnation point flow over an isothermal plate encompassed in a saturated porous medium, Makinde and Olanrewaju (2011) studied the effects of unsteadiness, chemical reaction, Dufour and Soret for a mixed convection boundary layer flow over a porous vertical plate moving through a binary mixture, which may be deemed of as an extension of Makinde et al. (2011) save the exclusion of thermal radiation characteristics, Olanrewaju and Gbadeyan (2011) analyzed a two-dimensional case with Soret, Dufour, chemical reaction effects in a porous medium. Olanrewaju and Adeniyan (2013) presented numerically, using similarity analysis, the effects of thermal-diffusion, diffusion-thermo and thermal radiation on a two-dimensional steady flow, heat and mass transfer due to a moving vertical plate placed in a saturated porous medium. They pointed out that mass transfer originating from the effect of temperature gradient finds utilization in isotope separation and in mixture between gases with medium molecular weight such as hydrogen-$air$ ($H_2, air$) and with very light molecular weight as in hydrogen-helium ($H_2$, He). Awad et al. (2011) investigated the heat and mass transfer characteristics in mixed convection along a semi-infinite stationary vertical plate in a porous medium with radiative heat transfer, diffusion-thermo and thermo-diffusion effects using successive linearization/Keller-box method. Makinde and Olanrewaju (2011) investigated the unsteady mixed convection flow past a vertical porous flat plate moving through a binary mixture in the presence of radiative heat transfer and n-th order Arrhenius type of irreversible chemical reaction by taking into account the diffusion thermal and thermo-diffusion effects. Later on, Olanrewaju et al. (2013) extended their work by incorporating the combined effects of an applied magnetic field and viscous dissipation.

Motivated by all the articles reviewed above, and in particular, for more physical implications, this present investigation extends in an obvious way the more recent works partaken by Bazid et al. (2012), Oahimire and Olajuwon (2013), Arthur and Seini (2014), and Adeniyan and Ogwuegbu (2014) with simultaneous inclusion of effects of temperature dependent thermal conductivity, the homogeneous first order chemical reaction, velocity slip, stress work, thermal-diffusion and diffusion-thermo, Lorentz and buoyancy forces along with exponentially decaying heat source for a hydromagnetic stagnation-point boundary layer flow towards a vertical permeable plate stretching linearly in an electrically conducting fluid; a rare find in the literature.

## 2. Mathematical Formulation

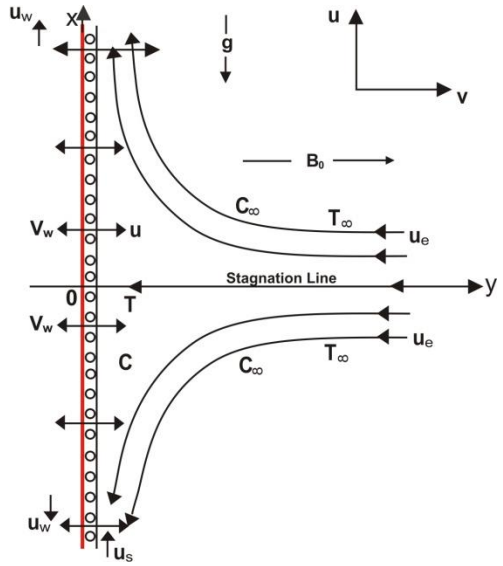


**Fig.** 1: Physical model and coordinate system

Let us consider a two-dimensional steady free convection stagnation flow, heat and mass transfer of a chemically reactive incompressible viscous fluid over a vertical permeable sheet stretching linearly in a saturated porous medium with velocity $u_w(\mathrm{x}) = b\mathrm{x}$ where $b > 0$ and x is a distance from a fixed (stagnation) point on the plate along the upward direction and $y \geq 0$ is the transverse distance directed into the entirety of the fluid as shown in Fig. 1. It is assumed that the ambient fluid is streaming with a velocity $u_e(\mathrm{x}) = a\mathrm{x}$, $a \geq 0$ such that the two velocities have the same direction. The velocity components of the fluid in the flow regime are $u(\mathrm{x},\mathrm{y})$ and $\mathrm{v}(\mathrm{x},\mathrm{y})$ respectively along the $\mathrm{x}-$ and $\mathrm{y}-$axes, while $\mathrm{v}_w$ represents the local wall mass flux velocity perpendicular to the plate such that $\mathrm{v_w} < 0$ is suction velocity and $\mathrm{v_w} > 0$ *is* injection velocity whereas $\mathrm{v}_w = 0$ is the condition for impermeability of the plate. In addition, the thermal conductivity of the fluid is temperature dependent and the property variations due to temperature and solute concentration are limited to the fluid density only. Ignoring Hall effects, and the magnetic Reynolds number. Taking into account the boundary-layer and Boussinesq approximations, the appropriate governing equations for mass , momentum, heat energy and species concentration balance in the presence of applied transverse magnetic field, and absence of an applied electric field are as stated herein:

$$\frac{\partial u}{\partial x} + \frac{\partial \mathrm{v}}{\partial y} = 0 \tag{1}$$

$$u\frac{\partial u}{\partial x} + \mathrm{v}\frac{\partial u}{\partial y} = u_e\frac{dU_e}{dx} + \nu\frac{\partial^2 u}{\partial y^2} + g\beta_T(T - T_\infty) + g\beta_C(C - C_\infty) - \frac{\sigma_e B_0^2}{\rho}(u - u_e) \tag{2}$$

$$u\frac{\partial T}{\partial x} + \mathrm{v}\frac{\partial T}{\partial y} = \frac{1}{C_P}u_e\frac{du_e}{dx}(u_e - u) + \frac{1}{\rho C_p}\frac{\partial}{\partial y}\left(k(T)\frac{\partial T}{\partial y}\right) + \frac{\dot{Q}^*}{\rho C_p} + \frac{D_m K_T \partial^2 C}{C_s C_p \partial y^2} \tag{3}$$

$$u\frac{\partial C}{\partial x} + \mathrm{v}\frac{\partial C}{\partial y} = D_m\frac{\partial^2 C}{\partial y^2} + \frac{D_m K_T}{T_m}\frac{\partial^2 T}{\partial y^2} - K_R(C - C_\infty) \tag{4}$$

subject to the boundary conditions:

$$\left.\begin{array}{l} \mathrm{v} = \mathrm{v}_w,\ u = u_w(\mathrm{x}) + u_s, T = T_w(\mathrm{x}),\ C = C_w(\mathrm{x})\ \ at\ y = o \\ u \to u_e(\mathrm{x}),\ \ T \to T_\infty, C \to C_\infty\ (\mathrm{x})\ as\ y \to \infty \end{array}\right\} \quad (5)$$

The temperature and the species concentration at the plate surface assume the following form:

$$T_w(\mathrm{x}) = T_\infty + cx^n,\ C_w(\mathrm{x}) = C_\infty + dx^n \quad (6)$$

c and d are constants and "n" is the exponent or power index of the wall temperature and concentration. (c has unit of temperature per n-th power distance, d has unit of concentration per n-th power distance) along the plate such that $T_W > T_\infty$ , $C_w > C_\infty$ respectively corresponding to heated plate and much loaded plate species concentration. In eq. (6) allowance has been made in the equal power-law indices for both wall temperature and concentration som that their ratio remains constant.

In the above equations (1) − (5), T, $T_\infty$ are fluid and free stream (ambient) temperatures, $C$, $C_\infty$ are species concentrations in the boundary layer and boundary edge, $T_w$, $C_w$ are the uniform wall temperature and species concentration. The acceleration due to gravity is $g$, where $\beta_T$ *and* $\beta_C$ are respective thermal and solutal expansivities, k(T) is the temperature dependent thermal conductivity of the fluid while $\nu$, $C_P$ and $\rho$ kinematic viscosity, specific heat at constant pressure and density of the fluid respectively. Also $\sigma_e$, is the electrical conductivity coefficient, $K_R$ is the chemical reaction rate constant, $K_T$ is the thermal diffusion ratio, $T_m$ is the mean fluid temperature, $C_s$ is the concentration susceptibility, $D_m$ is the coefficient of diffusivity due to mass (species concentration) transfer. The middle two terms of equation (1) involving $g$ represent the thermal and species concentration buoyancy forces respectively while the last stands for the Lorentz force. It is also assumed that the fluid contains a heat source $\dot{Q}^*$ which exhibits the property of exponential decay with the transverse dimensionless distance $\eta$ from the plate according to the laws given in equations (7), where the surface slip velocity is $u_s$ .

$$Q^* = Q_0(T_W - T_\infty)e^{-\eta},\ u_s = L\frac{\partial U}{\partial y}(x, 0) \quad (7)$$

In (7), L designates the slip length, $Q_0$ is the internal heat energy generation or absorption depending on whether $Q_0 > 0$ or $Q_0 < 0$.

Appropriate similarity variables/dimensionless parameters employed to transform the equations (1)-(5) above to ordinary boundary value problem are:

$$\left.\begin{array}{llll} \eta = y\sqrt{\frac{b}{\nu}}, & f(\eta) = \frac{\psi}{x\sqrt{b\nu}}, & \theta(\eta) = \frac{T-T_\infty}{T_w-T_\infty}, & \varepsilon = \frac{a}{b} \\ F_w = -\frac{v_w}{\sqrt{b\nu}}, & \lambda_T = \frac{Gc}{Re_x^2}, & \phi(\eta) = \frac{C-C_\infty}{C_w-C_\infty}, & Pr = \frac{\nu}{\alpha}, \\ Kr = \frac{K_R x^2}{\nu Re_x}, & Ha = \frac{\sigma_e B_0^2 x^2}{\mu Re_x}, & Sr = \frac{D_m K_T}{\nu T_m}\frac{T_w-T_\infty}{C_w-C_\infty}, & \delta = L\sqrt{\frac{b}{\nu}}, \\ Q = \frac{Q_0}{b\rho C_p}, & \lambda_T = \frac{Gr}{Re_x^2}, & Du = \frac{D_m K_{T(C_w-C_\infty)}}{C_s C_p(T_w-T_\infty)}, & Ec = \frac{{u_w}^2}{c_p(T_w-T_\infty)}, \\ & Re_x = \frac{x u_w(x)}{\nu}, & Gr = \frac{g\beta_T x^3(T_w-T_\infty)}{\nu^2} & Gc = \frac{g\beta_T x^3(C_w-C_\infty)}{\nu^2} \end{array}\right\} \quad (8)$$

In equations (8) above $\mu$ is the dynamic viscosity, Pr is the Prandtl number, $\varepsilon$ is the ratio of the velocity at wall to the velocity far off from the wall, Gr is the thermal Grashof number, Gc is the solutal Grashof number, $\lambda_T$ is the thermal buoyancy parameter while $\lambda_C$ is the solutal buoyancy parameter, Q is the internal heat energy generation parameter, $Re_x$ is the local Reynolds number, Sc is the Schmidt number, $Fw$ is the suction/injection (Fw $>$ 0 signifies suction and Fw $<$ 0 signifies injection, while Fw $=$0 is the case of impermeable sheet), $\eta$ is dimensionless transverse distance, $\psi$ is the dimensional stream function, $f(\eta)$ is dimensionless stream function, $\theta$ $and$ $\phi$ are dimensionless temperature an species concentration respectively, Ha is the Hartman number or magnetic parameter, $Du$ is the Dufour number, $Sr$ is the Soret number, Ec is the Eckert number, $Kr$ is the reaction rate parameter and $\delta$ is the velocity slip parameter. Following Hayat et al. (2014), the variation of thermal conductivity is discerningly taken as

$$k = k_\infty\left(1 + \beta\frac{T-T_\infty}{T_w-T_\infty}\right) \quad (9)$$

where $\beta$ is the parameter which depends on the nature of the fluid, called thermal conductivity variation parameter and $k_\infty$ is the value of the thermal conductivity at the free stream.

The velocity components in virtue of the stream function are

$$u = \frac{\partial\psi}{\partial y}, v = -\frac{\partial\psi}{\partial x} \quad (10)$$

which automatically accedes to the satisfaction of the equation (1) identically.
Using (7) and (9), and invoking (8) into the set of eqs. (2) − (4) alongside the boundary conditions (5), one gets the following set of non-similar equations, where " prime" designates ordinary differentiation with respect to $\eta$.

$$f''' + ff'' - (f')^2 - Ha(f' - \varepsilon) + \lambda_T\theta + \lambda_C\phi + \varepsilon^2 = 0 \quad (11)$$

$$\frac{I}{Pr}[(1+\beta\theta)\theta'' + \beta(\theta')^2] + f\theta' - nf'\theta + Qe^{-\eta} + Ec(\varepsilon - f') + Du\phi'' = 0 \qquad (12)$$

$$\frac{I}{SC}\phi'' + f\phi' - nf'\phi + Sr\theta'' - Kr\phi = 0 \qquad (13)$$

subject to the boundary conditions:

$$\left.\begin{array}{c} f(0) = Fw\,,\ f'(0) = 1 + \delta f''(0),\ \theta(O) = 1,\ \phi(0) = 1 \\ and\ f'(\infty) = \varepsilon,\ \theta(\infty) = 0,\ \phi(\infty) = 0 \end{array}\right\} \qquad (14)$$

In the absence of species concentration eq. (13), setting $\sigma = \ n = 1,\ F_w = \beta = \lambda_T = \lambda_C = Q = \delta = D_u = Ec = 0$ in our present equations (11)−(12) and (14), the result gives the set of equations due to Ishak et al. (2007). Further, setting $Fw = \delta = K = \lambda_C = D_u = Ec = S = 0$ in the same set of the resent work equations, one recovers another special case Bazid et al. (2012).

The local skin-friction coefficient $C_F$, the local Nusselt number $Nu_x$ and the local Sherwood number $Sh_x$, as important as the physical quantities of engineering interest, are defined in terms of wall shear stress $\tau_w$, heat exchange flux $q_w$, and mass flux at the wall $q_m$ as:

$$C_F = \frac{\tau_w}{\rho u_w^2},\ \ Nu_x = \frac{\mathrm{xq_w}}{k_\infty(\mathrm{T_w}-\mathrm{T_\infty})},\ Sh_x = \frac{xq_m}{D_m(C_w - C_\infty)} \qquad (15)$$

where

$$\tau_w = \mu\frac{\partial u}{\partial y}(\mathrm{x,o}),\quad q_w = -k\frac{\partial T}{\partial y}(x,y),\ q_m = -D_m\frac{\partial C}{\partial y}(x,0) \qquad (16)$$

and $\mu = \rho\nu$ is the dynamic viscosity.

Invoke (15) into (14), and then use (8)−(9) to obtain the dimensionless quantities

$$C_{Fr} = C_F Re_x^{\frac{1}{2}} = f''(0),\ Nur = Nu_x Re_x^{-\frac{1}{2}} = -(1+\beta)\theta'(0),\ \ \mathrm{Shr}=\mathrm{Sh_x Re_x^{-\frac{1}{2}}}=-\phi'(0) \qquad (17)$$

respectively called the reduced local skin-friction, reduced local Nulsselt number and reduced local Sherwood number which are measurable by $f''(0), -(1+\beta)\theta'(0),\ -\phi'(0)$.

## 3. Numerical procedure

The preceding set of equations (11) − (13) with the specified boundary conditions (14), after duly converted to systems of first order differential equations has been solved numerically using classical Runge-Kutta (R-K) integration algorithm alongside the Newton-Raphson (N-R) shooting quadrature (Abel et al., 2007; Ibrahim and Makinde, 2010, 2011; Akbar et al. 2014). Specifically, the selection of an appropriate value of the terminal point of the integration interval $[0, \eta_\infty]$ in place of $[0, \infty)$ is the crucial aspect in this method. To this end, we begin with the initial guesses of $f''(0),\ \theta'(0)\ and\ \phi'(0)$ and then the integration is carried out via R-K method. It is necessary to check the accuracy of the guesses by comparing with the given far field asymptotic values $f'(\infty)$, $\theta(\infty)$ and $\phi(\infty)$. The solution process is repeated with some smaller or larger guesses depending on their closeness to the boundary-edge values. If relative difference between the current and previous iterated guesses is pronounced the process is further repeated.

This iteration selection is achieved by means of N-R shooting method with difference error of $10^{-7}$, guaranteeing the convergence of the process and acceding its termination for accurate selection. In this work, a step size of $\Delta\eta = 0.001$ has been used for the numerical integration and $\eta_\infty = 9$ replaces $\eta \to \infty$ in nearly all cases and has been found satisfactory for a convergence criterion with accuracy to seven places of decimal. The implementation has been carried out on a computer programming language written in Maple-17. As these computations are default based there is need to attest the credibility of the computed results sorted out from the numerical process for values of the local skin friction coefficient $C_F$ or $f''(0)$, the reduced local Nusselt number Nur or $-\theta'(0)$, the reduced local Sherwood number Shr or $-\phi'(0)$ for selected numerical data obtained as special cases of previous published articles and thereafter we present our results in tables and figures for parametric variations.

## 4. Results and Discussion

### 4.1 Tabular Results

Table 1 reveals a comparison of this study for coefficient of friction with those of Ishak et al. (2007) who have used Keller-Box implicit finite difference scheme and Bazid et al. (2012) who have adopted fourth order Runge-Kutta integration scheme with Newton shooting method as aspecial cases using their basic flow parameter values. The presentation indicates a perfect agreement to four significant figures. Further comparison of the local skin friction and the reduced local Nusselt number is signposted in Table 3 with those of Bazid et al. (2012) for some selected parameter values, and again there is a positive affirmation of our computation codes. We bothered not to investigate the behavior of the fluid characteristics as per second or dual solutions which has been exhaustively tackled in the study of the latter, besides our investigation which centers on cooling processes in engineering and industrial applications exhibited by the positive values of the thermal convection parameter $\lambda_T$ along with the case for which the differences in species concentration between the plate surface and ambient values are positive corresponding to the positive values of the species concentration convection parameter $\lambda_C$. Furthermore, a comparison of the present work for the local skin friction, reduced local Nusselt and Sherwood numbers, as presented in Table 3 for some selected values of Bazid et al. (2012) specifically indicates an excellent agreement. Thusly, our computational method could be adduced trustworthy. Tables 4 and 5 delineate the computations of the local skin-friction coefficient, reduced local Nusselt number and reduced local Sherwood number for several values of the emerging flow parameters and highlighted for variation exhibition. As it can be viewed from these tables, the local skin-friction coefficient, reduced local Nusselt number and reduced local Sherwood number all increase in values as the buoyancy parameters $(\lambda_T,\ \lambda_C)$ as well as suction parameter $(Fw > 0)$ are increased. The trio $(f''(0), -(1+\beta)\theta'(0), -\phi'(0))$ decrease in values with increasing magnitudes of either of

the magnetic parameter ($Ha$) or injection parameter ($Fw < 0$). More importantly, it is worthy to note that the local skin-friction generally increases with an increase in magnetic field and injection parameters. Also one notices that both the local wall shear stress and the local species mass flux at the plate surface increase in values as the thermal conductivity variation parameter ($\beta$) increases, but opposite trend is recorded as the Prandtl number (Pr) increases in values. However, the reduced local Nusselt number can be increased in values consequential to increase in Pr, and be decreased in values as $\beta$ improves in values. It is quite interesting as observed in the Tables 4-5, that increase in exponent parameter (n) in its effect decreases the values of the local skin friction coefficient but causes increment in the magnitudes of the reduced local Nusselt snd the Sherwood numbers respectively. As revealed from these tables, again both the local skin-friction coefficient and the reduced local Sherwood number increase in magnitudes as the internal heat energy parameter (Q) intensifies whereas the reverse is the case for the reduced local Nusselt number. Further, the local skin-friction coefficient and the reduced local Sherwood number decrease in values as Eckert number advances in magnitudes while the opposite is seen in the case of the reduced local Nusselt number. It is, however noteworthy that the concurrence of variation of the Dufour number (while decreasing) and Soret number (while increasing) consequentially influences the magnitude variation of not only the reduced local skin-friction coefficient and local Nusselt number but also the reduced local Sherwood number. The combined variation as it increases, causes increment in both ($C_F \; or \; f''(0) \; and \; Nur \; or \; -(1+\beta)\theta'(0)$) but a decrease in ($Shr \; or \; -\phi'(0)$). Tables 4-5 unveil that both the local skin-friction coefficient and the reduced local Nusselt number diminish in values as each of the Schmidt number (Sc) and chemical reaction (Kr) parameters intensify in magnitude. But of course, the reverse trend is signposted by the Sherwood number. Specifically, increasing the values of the velocity slip parameter ($\delta$) results into a reduction in the values of the local skin-friction coefficient and a magnification in the values of both the reduced local Nusselt and Sherwood numbers anyway. As important as it, is the influence of the stretching parameter on the local wall velocity gradient $C_F$, heat transfer rate $Nur$ and species concentration transfer rate $Shr$ at the wall. One notices from the tables that the flow, heat and mass transfer characteristics at the wall all increase as the stretching parameter ($\sigma$) increases, besides the reduced local skin-friction coefficient which increases absolutely. However, it is observed that the values of the local skin friction are negative for this special case. Of course, the negative value of the skin-friction physically means that the dragging force is being exerted on the fluid as opposed to the usual case of dragging force being exerted on the wall by the fluid.

## 4.2 Graphical Results

### 4.2.1 Effect of parameter variation on velocity field

Figs. $2-10$ depict the velocity profiles $f(\eta)$ against the transverse distance $\eta$ for a range of values of the governing flow parameters. The velocity distribution assumes its wall value and varies continuously to attain the boundary edge value asymptotically, in general. Specifically, as illustrated in these figures, the variation indicates an overshot near the wall for some cases, thereafter it nosedives to the far field value. It may be worthy to mention that due to lack of space some of our figures with almost similar variations have been omitted and retained their representatives. Fig. 2 serves as a representative velocity plot for Pr, Sc, Ec, Kr and n variations while Fig. 3 is an approximate representative revealing similar velocity plot for the variations in $\lambda_c$ and $\beta$. Particular attention is paid to the dual velocity distributions as demonstrated for value variation of the stretching parameter ($\sigma$) in Fig. 7 together with velocity slip parameter ($\delta$) Fig. 8 wherein the velocity increases at first before a cross point in the boundary layer and opposite trend emanates thereafter. Interestingly, it can be reported that the dimensionless velocity increases with an increase in parameter values of $\lambda_T,\ \lambda_C,\ \mathcal{E},\ \beta,\ Q,\ Ec,\ Sc,\ Kr,$ injection ($Fw < 0$), $\delta$ and σ (before the cross point), Du (decreasing) and Sr (increasing) concurrently, but decreases with an increase in $Ha,\ Pr,\ n,$ suction ($Fw > 0$), $\delta$ and σ (after the cross point). Thusly, not only the Lorentz forces exhibited by magnetic parameter (Ha), inhibit the fluid velocity but also the Prandtl number (Pr) and the exponent parameter (n). These parameters may be recommended for velocity boundary layer speed control. Further, the buoyancy forces due to temperature and concentration differences as well as the Prandtl and Schmidt numbers (Pr, Sc), thermal conduction variation and chemical reaction parameters ($\beta, Kr$) can accelerate the fluid velocity in a boundary layer flow which in consequence may promote boundary layer separation.

### 4.2.2 Effect of parameter variation on temperature field

The variations of temperature distribution for a range of basic flow parameters are demonstrated in representative Figs. $11-16$, where as observed, the wall value boundary condition is satisfactorily fulfilled and the far field condition is attained asymptotically. However, the fluid temperature decreases in the thermal boundary layer as nearly all flow controlling parameters increase, except the case of increasing the magnetic, heat generation and injection parameters which show contrary influence. The thermal distribution features in each of the figures an observable decay in magnitude in the boundary layer, save the case of the variation in Q, as noticed in Fig. 13 which emanates a peak value near the plate. In particular, the high temperature recorded near the plate surface may be detrimental to the quality of penultimate products in some engineering and industrial processes. Therefore there is need for temperature control in fluid boundary layer flow harboring heat energy generation. As it can be seen in Fig. 11, the temperature distribution increases appreciably consequential upon increment in the magnetic field parameter, and similar variation (omitted) was recorded for Schmidt number (Sc), thermal

conduction variation ($\beta$) and chemical reaction (Kr) parameters. The respond of the thermal distribution with the dimensionless transverse distance $\eta$ as presented in Figure 12 unveils a monotonic decrease in the fluid temperature everywhere in the thermal boundary layer as the Prandtl number (Pr) strengthens in magnitude. Again, almost similar response, though omitted for obvious reasons stated earlier, has been recorded for each of the cases for which the parameters $\lambda_T$, $\lambda_C$, $\mathcal{E}$, n, $\sigma$, $\delta$ intensify in magnitudes. The variation of the temperature profiles with respect to suction/injection parameter is signposted by Fig. 15. Clearly, the dimensionless fluid temperature increases in values as the injection parameter (Fw<0) increases but reverse is the response recoded for increasing suction parameter (Fw>0). Thusly, this study also reaffirms that suction mechanism can be used as a means of temperature control within the thermal boundary layer. The revelation as presented in Fig. 14 is quite astonishing in the sense that the fluid temperature is reduced by combined Du (decreasing) and Sr (increasing) concurrently and oncemore, a confirmation of earlier report of Bazid et al. (2012). Particular attention is focused on the influence of the stress work which is characterized by the Eckert number (Ec) whose increment causes fluid temperature reduction, see Fig. 16. It therefore follows that the energy due to fluid interaction at the surface without the interaction of the fluid friction enhances temperature reduction.

### 4.2.3 Effect of parameter variation on concentration field

Figs. 17 − 19 show selected profiles of the species concentration versus $\eta$ for various values of the basic flow parameters in the boundary layer regime. As demonstrated in all the figures, the species concentration, starting from the largest wall value depreciates monotonically within the boundary layer to assume the asymptotic free stream value of zero. Clearly, as noticed for the parametric variation on the concentration profiles ( some figures are omitted due to space economy), increase in the flow controlling parameters of suction, ( $Fw > 0$) , $\lambda_T$, $\lambda_C$, $\mathcal{E}$, $n$, $Sc$, $Ec$, $Kr$, $\sigma$, $\delta$ significantly decreases the concentration of species while increase in injection (Fw<0) and magnetic field (Ha) parameters considerably leads to a depletion in the concentration boundary layer thickness. In addition, a further concurrent increase in combined Du(decreasing) and Sr (increasing) leads to a reduction in concentration of species. This again is in agreement with observation presented by Bazid et al. (2012). Also it is found that increase in heat generation and thermal conductivity variation parameters is inconsequential in its effect on concentration distribution at each location of the boundary layer and we border not to present them. The effects observed due to the Prandtl number (Pr) and the heat generation parameter (Q) are very minimal and their plots are not included. It is found that the concentration profiles increase very mildly as Pr increases whereas the opposite trend prevails, also mildly as Q increases.

## 5. Table and Figure Legends

**Table 1:** Computations showing comparison of the local skin-friction coefficient $f''(0)$ , with Ishak et al. [2007] and Bazid et al. [2012] results when $Pr = \sigma = \ n = 1,\ F_w = \beta = \lambda_T = \lambda_C = Q = Sc = \delta = D_u = S_r = Ec = 0$

| ε | Ishak et al. [2007] | Bazid et al. [2012] | Present |
|---|---|---|---|
| | $f''(0)$ | | |
| 0.1 | -0.9694 | -0.9694 | -0.969386157 |
| 0.2 | -0.9181 | -0.9181 | -0.918107137 |
| 0.5 | -0.6673 | -0.6673 | -0.667263671 |
| 2 | 2.0175 | 2.0175 | 2.017502802 |
| 3 | 4.7294 | 4.7292 | 4.729282356 |

**Table 2:** Computations showing comparison of the local skin-friction coefficient $f''(0)$ and reduced local Nusselt number $-(1+\beta)\theta'(0)$, Bazid et al. [2012] results when $Pr = \lambda_T = \sigma = \ n = 1,\ F_w = \beta = \lambda_C = Q = Sc = \delta = D_u = S_r = Ec = 0$

| Pr | Bazid et al. [2012] | | Present | |
|---|---|---|---|---|
| | $f''(0)$ | $-\theta'(0)$ | $f''(0)$ | $-\theta'(0)$ |
| 0.72 | 0.3645 | 1.0931 | 0.364492792 | 1.093108 |
| 6.8 | 0.1804 | 3.2894 | 0.180415289 | 3.289574 |
| 20 | 0.1173 | 5.6182 | 0.117500107 | 5.620131 |
| 40 | 0.0845 | 7.9383 | 0.087242479 | 7.938306 |
| 60 | 0.0682 | 9.7141 | 0.07284223 | 9.718013 |
| 80 | 0.0572 | 11.2205 | 0.063942409 | 11.21874 |
| 100 | 0.0491 | 12.5829 | 0.057727598 | 12.5411 |

**Table 3:** Computations showing comparison of the local skin-friction coefficient $f''(0)$, reduced local Nusselt number $-(1+\beta)\theta'(0)$, reduced local Sherwood number $-\phi'(0)$, with Bazid et al. [2012] results when $Sc = \lambda_T = \sigma = \varepsilon = \ n = 1,\ \beta = 0.4,\ F_w = \lambda_C = Q = \delta = D_u = S_r = Ec = 0$

| Flow parameters With different values | | | Bazid et al. [2012] | | | Present | | |
|---|---|---|---|---|---|---|---|---|
| Pr | Du | Sr | $f''(0)$ | $-\theta'(0)$ | $-\phi'(0)$ | $f''(0)$ | $-\theta'(0)$ | $-\phi'(0)$ |
| 0.72 | 0.3 | 0.2 | 0.5761 | 0.7844 | 1.2552 | 0.576125 | 0.784419 | 1.255237 |
| 0.72 | 0.12 | 0.5 | 0.5735 | 0.8532 | 1.1522 | 0.573481 | 0.853188 | 1.152245 |
| 0.72 | 0.08 | 0.75 | 0.5785 | 0.8691 | 1.0675 | 0.578478 | 0.869118 | 1.067484 |
| 0.72 | 0.3 | 0.2 | 0.5761 | 0.7844 | 1.2552 | 0.576125 | 0.784419 | 1.255237 |
| 1 | 0.3 | 0.2 | 0.5511 | 0.9116 | 1.235 | 0.551139 | 0.911593 | 1.234975 |
| 3 | 0.3 | 0.2 | 0.4714 | 1.5373 | 1.1289 | 0.471379 | 1.537357 | 1.128877 |

**Table 4:** Computations showing the local skin friction coefficient $C_F$ *or* $(f''(0))$, reduced local Nusselt number Nur or $(-(1+\beta)\theta'(0))$ and reduced local Sherwood number $Shr$ *or* $(-\phi'(0))$ for various emerging flow parameter values

| Ha | $\lambda_T$ | $\lambda_C$ | ε | Pr | β | n | Q | $C_F$ | Nur | $Shr$ |
|---|---|---|---|---|---|---|---|---|---|---|
| 0.1 | 0.1 | 0.1 | 0.1 | 0.72 | 0.1 | 0.1 | 0.1 | 0.19601723 | 0.31819186 | 0.24891860 |
| 1 | 0.1 | 0.1 | 0.1 | 0.72 | 0.1 | 0.1 | 0.1 | 0.13212210 | 0.27301334 | 0.23681552 |
| 3 | 0.1 | 0.1 | 0.1 | 0.72 | 0.1 | 0.1 | 0.1 | 0.08477867 | 0.23986812 | 0.22880468 |
| 0.1 | 0.1 | 0.1 | 0.1 | 0.72 | 0.1 | 0.1 | 0.1 | 0.19601723 | 0.31819186 | 0.24891860 |
| 0.1 | 0.5 | 0.1 | 0.1 | 0.72 | 0.1 | 0.1 | 0.1 | 0.47204767 | 0.40618804 | 0.27473781 |
| 0.1 | 1 | 0.1 | 0.1 | 0.72 | 0.1 | 0.1 | 0.1 | 0.75652574 | 0.47168126 | 0.29564286 |
| 0.1 | 0.1 | 0.1 | 0.1 | 0.72 | 0.1 | 0.1 | 0.1 | 0.19601723 | 0.31819186 | 0.24891860 |
| 0.1 | 0.1 | 0.5 | 0.1 | 0.72 | 0.1 | 0.1 | 0.1 | 0.51018925 | 0.43517126 | 0.28525428 |
| 0.1 | 0.1 | 1 | 0.1 | 0.72 | 0.1 | 0.1 | 0.1 | 0.83796690 | 0.51892333 | 0.31479958 |
| 0.1 | 0.1 | 0.1 | 0.1 | 0.72 | 0.1 | 0.1 | 0.1 | 0.19601723 | 0.31819186 | 0.24891860 |
| 0.1 | 0.1 | 0.1 | 1 | 0.72 | 0.1 | 0.1 | 0.1 | 1.21558606 | 0.55589664 | 0.39455855 |
| 0.1 | 0.1 | 0.1 | 2 | 0.72 | 0.1 | 0.1 | 0.1 | 3.16375727 | 0.77699246 | 0.52539536 |
| 0.1 | 0.1 | 0.1 | 0.1 | 0.72 | 0.1 | 0.1 | 0.1 | 0.19601723 | 0.31819186 | 0.24891860 |
| 0.1 | 0.1 | 0.1 | 0.1 | 1 | 0.1 | 0.1 | 0.1 | 0.19086406 | 0.36930357 | 0.24553504 |
| 0.1 | 0.1 | 0.1 | 0.1 | 3 | 0.1 | 0.1 | 0.1 | 0.17371672 | 0.61562504 | 0.23198300 |
| 0.1 | 0.1 | 0.1 | 0.1 | 0.72 | 0.1 | 0.1 | 0.1 | 0.19601723 | 0.31819186 | 0.24891860 |
| 0.1 | 0.1 | 0.1 | 0.1 | 0.72 | 0.5 | 0.1 | 0.1 | 0.20029573 | 0.35801968 | 0.25215926 |
| 0.1 | 0.1 | 0.1 | 0.1 | 0.72 | 1 | 0.1 | 0.1 | 0.20437390 | 0.40309225 | 0.25483762 |
| 0.1 | 0.1 | 0.1 | 0.1 | 0.72 | 0.1 | 0.1 | 0.1 | 0.19601723 | 0.31819186 | 0.24891860 |
| 0.1 | 0.1 | 0.1 | 0.1 | 0.72 | 0.1 | 0.5 | 0.1 | 0.18937797 | 0.38255088 | 0.27811859 |
| 0.1 | 0.1 | 0.1 | 0.1 | 0.72 | 0.1 | 1 | 0.1 | 0.18255563 | 0.44992513 | 0.31017921 |
| 0.1 | 0.1 | 0.1 | 0.1 | 0.72 | 0.1 | 0.1 | 0.1 | 0.19601723 | 0.31819186 | 0.24891860 |
| 0.1 | 0.1 | 0.1 | 0.1 | 0.72 | 0.1 | 0.1 | 0.5 | 0.20468354 | 0.0953347 | 0.25988273 |
| 0.1 | 0.1 | 0.1 | 0.1 | 0.72 | 0.1 | 0.1 | 1 | 0.21513190 | -0.1819372 | 0.27339809 |

**Table 5:** Computations showing the local skin-friction coefficient $C_F$ *or* $(f''(0))$, reduced local Nusselt number Nur or $(-(1+\beta)\theta'(0))$ and reduced local Sherwood number Shr or $(-\phi(0))$ for various emerging flow parameter values

| Ec | Du | Sc | Sr | Kr | Fw | σ | δ | $C_F$ | Nur | $Shr$ |
|---|---|---|---|---|---|---|---|---|---|---|
| 0.1 | 0.3 | 0.24 | 0.2 | 0.1 | 0.1 | 0.1 | 0.1 | 0.1960172 | 0.3181918 | 0.2489186 |
| 0.5 | 0.3 | 0.24 | 0.2 | 0.1 | 0.1 | 0.1 | 0.1 | 0.1897870 | 0.3936260 | 0.2442644 |
| 1 | 0.3 | 0.24 | 0.2 | 0.1 | 0.1 | 0.1 | 0.1 | 0.1828334 | 0.4767947 | 0.2390642 |
| 0.1 | 0.3 | 0.24 | 0.2 | 0.1 | 0.1 | 0.1 | 0.1 | 0.1960172 | 0.3181918 | 0.2489186 |
| 0.1 | 0.12 | 0.24 | 0.5 | 0.1 | 0.1 | 0.1 | 0.1 | 0.1961591 | 0.3343742 | 0.2369918 |
| 0.1 | 0.08 | 0.24 | 0.75 | 0.1 | 0.1 | 0.1 | 0.1 | 0.1971073 | 0.3389530 | 0.2271988 |
| 0.1 | 0.3 | 0.5 | 0.2 | 0.1 | 0.1 | 0.1 | 0.1 | 0.1867627 | 0.2877468 | 0.3594124 |
| 0.1 | 0.3 | 1 | 0.2 | 0.1 | 0.1 | 0.1 | 0.1 | 0.1764786 | 0.2468934 | 0.5237048 |
| 0.1 | 0.3 | 0.24 | 0.2 | 0.1 | 0.1 | 0.1 | 0.1 | 0.1960172 | 0.3181918 | 0.2489186 |
| 0.1 | 0.3 | 0.24 | 0.2 | 0.5 | 0.1 | 0.1 | 0.1 | 0.1861918 | 0.2807590 | 0.3959259 |
| 0.1 | 0.3 | 0.24 | 0.2 | 1 | 0.1 | 0.1 | 0.1 | 0.1789598 | 0.2482745 | 0.5283861 |
| 0.1 | 0.3 | 0.24 | 0.2 | 0.1 | -0.3 | 0.1 | 0.1 | 0.1804606 | 0.1780058 | 0.2062373 |
| 0.1 | 0.3 | 0.24 | 0.2 | 0.1 | -0.1 | 0.1 | 0.1 | 0.1893078 | 0.2429561 | 0.2270228 |
| 0.1 | 0.3 | 0.24 | 0.2 | 0.1 | 0 | 0.1 | 0.1 | 0.1929519 | 0.2793399 | 0.2378263 |
| 0.1 | 0.3 | 0.24 | 0.2 | 0.1 | 0.1 | 0.1 | 0.1 | 0.1960172 | 0.3181918 | 0.2489186 |
| 0.1 | 0.3 | 0.24 | 0.2 | 0.1 | 0.3 | 0.1 | 0.1 | 0.2003073 | 0.4027884 | 0.2720191 |
| 0.1 | 0.3 | 0.24 | 0.2 | 0.1 | 0.1 | 0.5 | 0.1 | -0.1788277 | 0.4344585 | 0.2790141 |
| 0.1 | 0.3 | 0.24 | 0.2 | 0.1 | 0.1 | 1 | 0.1 | -0.7897420 | 0.5500105 | 0.3102570 |
| 0.1 | 0.3 | 0.24 | 0.2 | 0.1 | 0.1 | 0.1 | 0.1 | 0.1960172 | 0.3181918 | 0.2489186 |
| 0.1 | 0.3 | 0.24 | 0.2 | 0.1 | 0.1 | 0.1 | 0.5 | 0.1484270 | 0.3374051 | 0.2538020 |
| 0.1 | 0.3 | 0.24 | 0.2 | 0.1 | 0.1 | 0.1 | 1 | 0.1127780 | 0.3505541 | 0.2571640 |

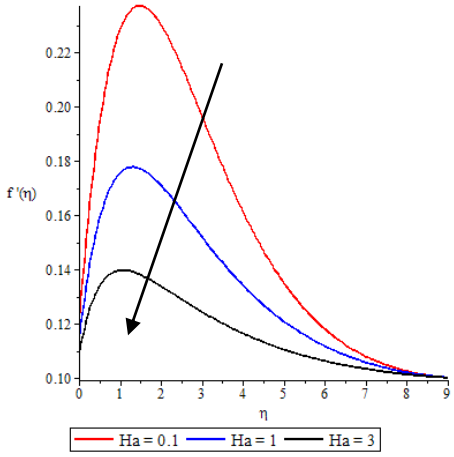


**Fig. 2**: Effect of Ha on velocity profiles

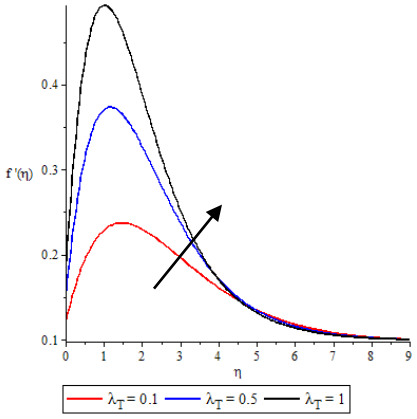


**Fig. 3**: Effect of $\lambda_T$ on velocity profiles

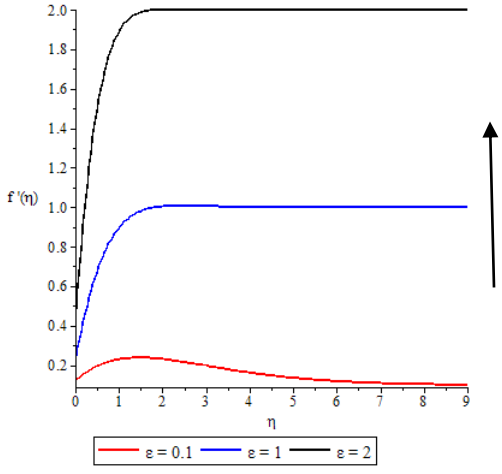


**Fig. 4**: Effect of $\mathcal{E}$ on velocity profiles

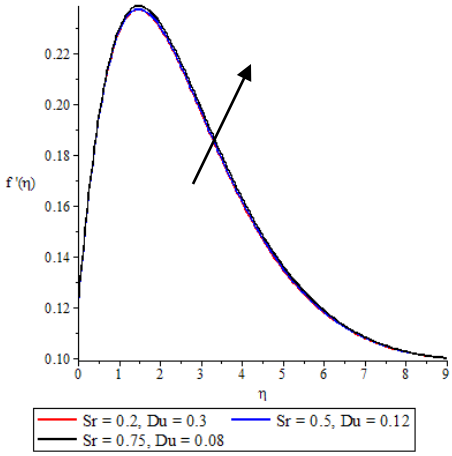


**Fig. 5**: Effects of Sr and Du on the velocity profiles

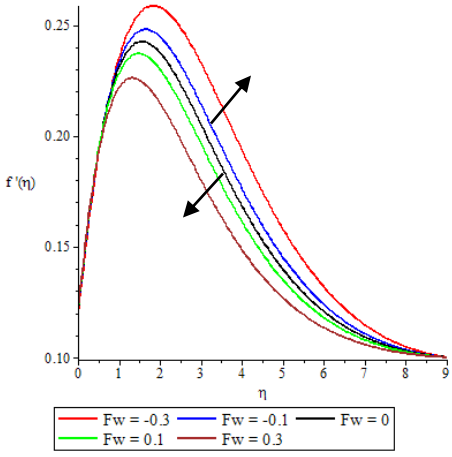


**Fig. 6**: Effect of $Fw$ on velocity profiles

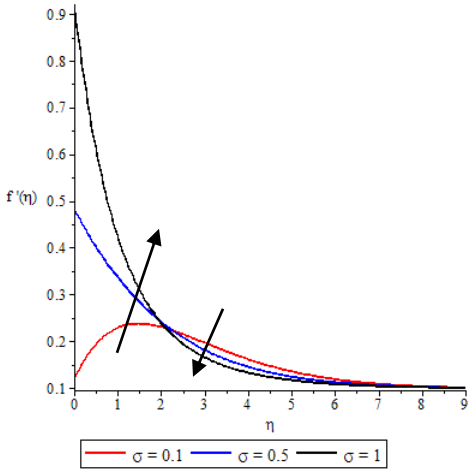


**Fig. 7**: Effect of $\sigma$ on velocity profiles

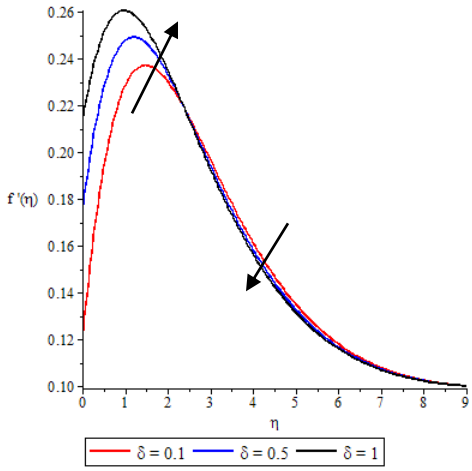


**Fig. 8**: Effect of $\delta$ on velocity profiles

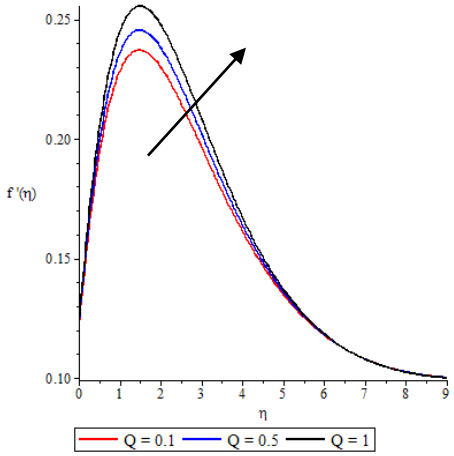


**Fig. 9**: Effect of $Q$ on velocity profiles

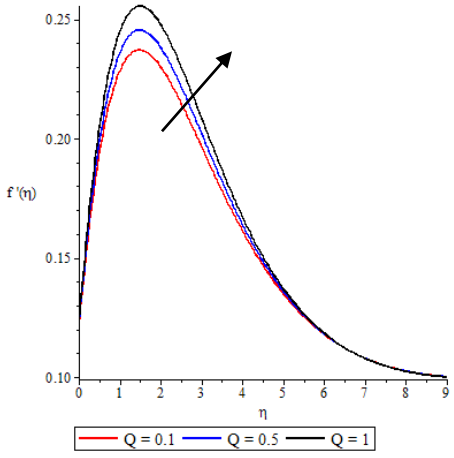


**Fig. 10**: Effect of $Q$ on velocity profiles

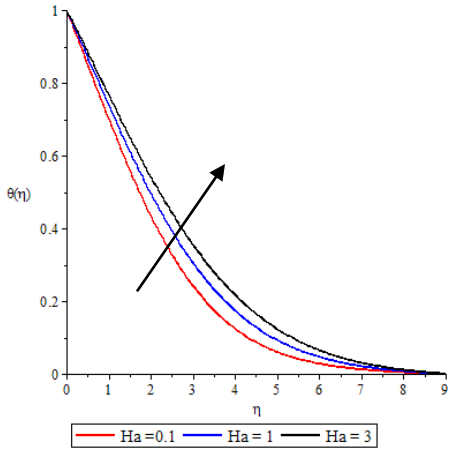


**Fig. 11**: Effect of $Ha$ on temperature profiles

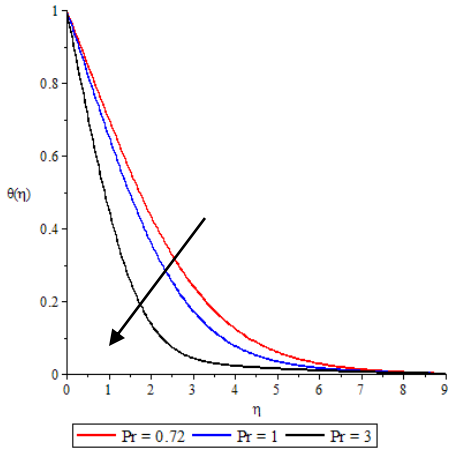


**Fig. 12**: Effect of $Pr$ on temperature profiles

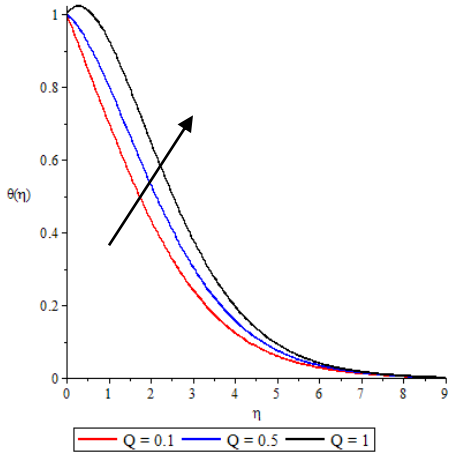


**Fig. 13**: Effect of $Q$ on temperature profiles

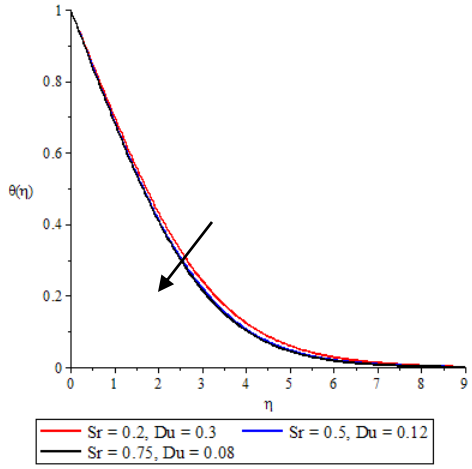


**Fig. 14**: Effects of Sr and Du on temperature profiles

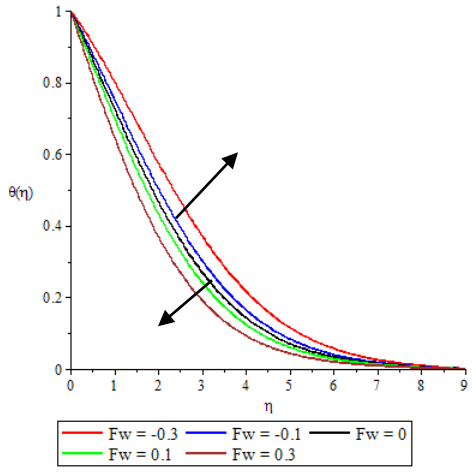


**Fig. 15**: Effect of $Fw$ on temperature profiles

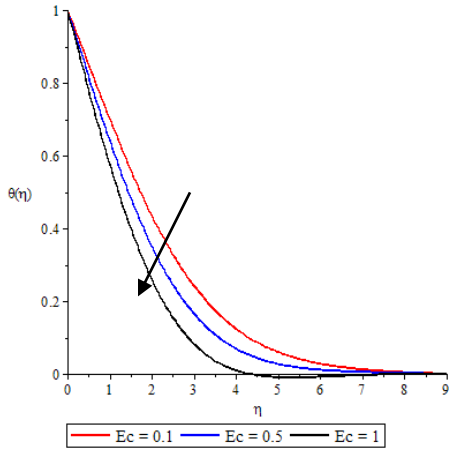


**Fig. 16**: Effect of $Ec$ on temperature profiles

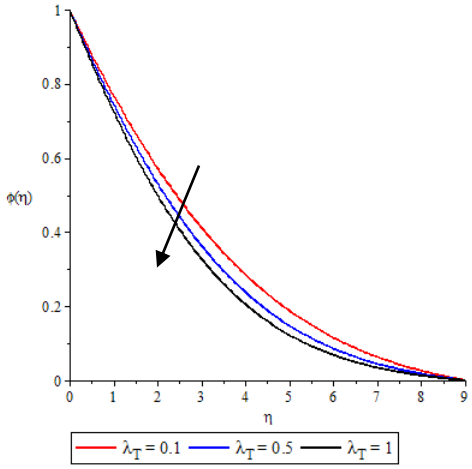


**Fig. 17**: Effect of $\lambda_T$ on concentration profiles

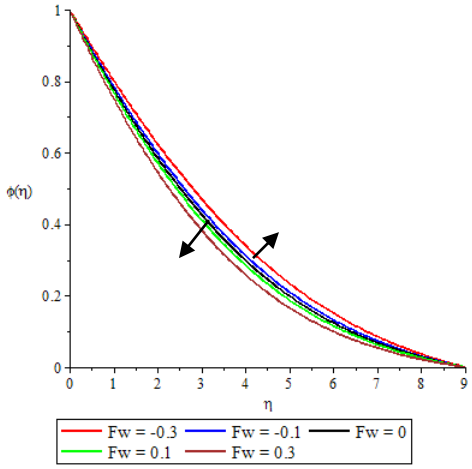


**Fig. 18**: Effect of $Fw$ on concentration profiles

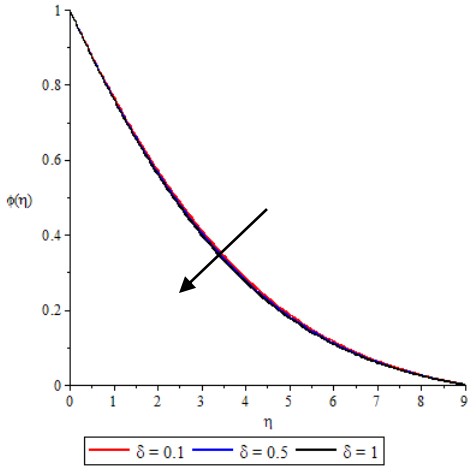


**Fig. 19**: Effect of $\delta$ on concentration profile

## 6. Conclusions

Investigation has been carried out numerically to study the heat and mass transfer characteristics of a chemically reacting hydromagnetic flow towards a permeable stretching vertical plate awash of a transverse magnetic field in the presence of buoyancy forces, stress work, heat generation, suction/injection, thermal conductivity variation, Dufour and Soret effects. The results of our findings are as follows:

1. The local velocity gradient, the local heat and mass transfer rates at plate surface increase as buoyancy parameters $(\lambda_T, \lambda_C)$ and velocity ratio $(\mathcal{E})$ increase.
2. The fluid velocity increases everywhere in the momentum boundary layer as buoyancy parameters $(\lambda_T, \lambda_C)$, Eckert and Schmidt numbers $(Ec, Sc)$, velocity ratio $(\mathcal{E})$, thermal conductivity variation $(\beta)$, heat generation $(Q)$ and chemical reaction $(Kr)$ parameters increase.
3. The local skin friction coefficient and the reduced local Nusselt number increase due to increase in suction $(Fw > 0)$ as well as concurrent variation in $Du$ (decreasing) and Soret (increasing).
4. The local velocity gradient, the heat and mass transfer local rates at plate surface decrease as the injection $(Fw < 0)$ and magnetic (Ha) parameters increase, but increase with increase in the stretching parameter $(\sigma)$.
5. The local skin friction coefficient and the fluid velocity are reduced by increase in the magnetic field parameter $(Ha)$ whereas fluid temperature and concentration of species are increased by increase in Ha.
6. The reduced local Nusselt and local Sherwood numbers can be increased by increasing the values of temperature/concentration exponent $(n)$ and stretching $(\sigma)$ parameters while the dimensionless thermal and solutal distributions are reducible by increasing the stretching parameter $(\sigma)$.
7. The heat transfer local rate at the wall can be increased by increase in Pr whereas the mass transfer local rate at the wall demonstrates opposite trend.
8. The heat transfer local rate can be decreased by increase in Sc as well as Q and Kr, whereas the mass transfer local rate at the wall demonstrates opposite trend.
9. The temperature field increases as Sc and Kr intensify in values while the reverse is unveiled as Sc and Kr intensify.
10. The temperature field can be decreased by increase in $(Ec, Pr, \delta)$ whereas concurrent variation in $Du$ (decreasing) and Soret (increasing) decreases the local Nusselt number and increases the local Sherwood number, but the temperature and concentration of species are respectively decreased and increased by concurrent variation in $Du$ (decreasing) and Soret (increasing).

## Acknowledgments

The author wishes to thank the University of Lagos for provision of books, referred articles and computer facilities.

## REFERENCES

[1] Abel, M. S. and Mahesha, N. (2008). Heat transfer in MHD viscoelastic fluid flow over a stretching sheet with variable thermal conductivity, non-uniform heat source and radiation, *Appl. Math. Modelling.* **32**, pp. 1965-1983.

[2] Adeniyan, A. and Adigun, J. A. (2014). Transient MHD boundary-layer slip-flow of heat and mass transfer over a stretching surface embedded in porous medium with waste discharge concentration and convective boundary conditions. *Applied and Computational Mathematics.* **3**, (5), pp. 247-255. doi: 8/j.acm.20140305.19.

[3] Adeniyan, A. and Adigun, J. A. (2013). Studies of effects of convective plane stagnation point Mhd flow with convective boundary condition in the presence of a uniform magnetic field. *Int. J. Eng. Sci.*, **2**, (1), pp. 310-313.

[4] Adeniyan, A. and Ogwuegbu, C. S. (2014). Effects of chemical reaction and heat generation on a mixed convection stagnation point flow, heat and mass transfer towards a stretching vertical porous flat plate. *Asian Research Publishing Network [ARPN] J. Engng. & Appl. Sci.* **9**, (12), pp. 2676-2686.

[5] Adrian, P. (2010). Heat and mass transfer by natural convection at a stagnation point in a porous medium considering Soret and Dufour effects. *Heat Mass Transfer*. **46**, pp 831 – 840.

[6] Akbar, N. S., Khan, Z. H., Haq, R. U., Nadeem, S. (2014). Dual solutions in MHD stagnation point flow of Prandtl fluid impinging on shrinking sheet, *Appl. Math. & Mech.* (*Engl. Ed.),* pp. 1-7.

[7] Aman, F., Ishak, A. and Pop, I. (2011). Mixed convention boundary layer flow near stagnation-point on vertical surface with slip. *Appl. Math. Mech. Engl. Ed*. **32**, (12), pp. 1599-1606.

[8] Anderson, J. D. (2005). Ludwig Prandtl's boundary layer. *American Institute of Physics, Physics Today*-S-0031-9228-0512-020-1.

[9] Arthur, E. M. and Seini, Y. I. (2014). MHD thermal stagnation point flow towards a stretching porous surface. *Mathematical Theory & Modeling*. **4**, (5), pp. 163-179.

[10] Awad, F. G., Sibanda, P., Narayana, M., Motsa, S. S. (2011). Convection from a semi-infinite plate in a fluid saturated porous medium with cross-diffusion and radiative heat transfer, *Int. Journ. Phys. Sciences*. **6** (21), pp. 4910-4923.

[11] Bazid, M. A. A., Gharsseldieu, Z. M., Seddeek, M. A., Alharbi, M. (2012). Soret and Dufour number effect on heat and mass transfer in stagnation point flow towards a stretching surface in the presence of buoyancy force and variable thermal conductivity, *Journ. of Computations & Modelling*. **2**, (4), pp. 25-50.

[12] Bhattacharyya, K and Mukhopadhyay, S. (2013). Similarity solution of mixed convective boundary layer slip flow over a vertical plate. *Ain Shams Engng. J.* 4, 299-305.

[13] Chen, H. (2014). Mixed convection unsteady stagnation-point flow towards a stretching sheet with slip effects. *Mat. Prob. Eng.* Article ID 435697, pp. 1-7.

[14] Crane, L. J. (1970). Flow past a stretching plate, Z. *Angew. Math. Phys*. **21**, 645-647

[15] Eegunjobi, A. S. and Makinde, O. D. (2012). Combined effect of buoyancy force and Navier slip on entropy generation in a vertical channel. *Entropy*. **14**, pp. 1028-1044.

[16] Usman, H. and Uwanta, J. I. (2013). Effect of thermal conductivity on Mhd heat and mass transfer flow past an infinite vertical plate with Soret and Dufour effects. *American Journal of Applied Mathematics.* Vol. 1. No. 3, 2013, pp. 28-38

[17] Hayat, T., Shehzad, S. A., Qasim, M., Alsaedi, A. (2014). Mixed convection flow by a porous sheet with variable thermal conductivity and a convective boundary condition. *Brazilian J. of Chem. Eng*. 31, (1), pp. 109-117.

[18] Hiemenz, K. (1911). Die Grenzschicht an eimen in den gleichformigen Flussignkeitsstrom eingetauchten geraden Kreiszylinder Dingl. *Polytech. J*. 32, 321-410.

[19] Ibrahim, S. M. and Reddy, N. (2013). Similarity solution of heat and mass transfer for natural convection over a moving vertical plate with internal heat generation and a convective boundary condition in the presence of thermal radiation, viscous dissipation, and chemical reaction. *Thermodynamics*, Article ID 790604, pp. 1-10.

[20] Ibrahim, S. Y. and Makinde, O. D. (2010). Chemically reacting MHD boundary layer flow of heat and mass transfer over a moving vertical plate with suction. *Scientific Research and Essays*, 5 (19), pp. 2875-2882.

[21] Ibrahim, S. Y and Makinde, O. D (2011), Chemically reacting Magnetohydrodynamics (MHD) boundary layer flow of heat and mass transfer past a low-heat-resistant sheet moving vertically downwards, Scientific Research and Essays, vol. 6(22), pp. 4762-4775

[22] Ishak, A., Nazar, R., Arifin, N. M., Pop, I. (2007). Mixed convection of a stagnation point flow towards a stretching permeable sheet. *Malaysian Journal of Mathematical sciences* . 1 (2), pp. 217-226.

[23] Joshi, Y. and Gebhart, B. (1981). Effect of pressure stress work and viscous dissipation in some natural convection flow. *Int. J. of Heat and Mass Transfer*. 24, pp. 1577-1588.

[24] Khan, S. K., Abel, M. S., Sonth, R. M. (2003). Viscoelastic MHD flow, heat and mass transfer over a porous stretching sheet with dissipation energy and stress work. *Heat and Mass Ttransfer*. 40, pp. 47-53.

[25] Mahapatra, T. R., Nandy, S. K. (2013). Momentum and heat transfer in MHD axisymmetric stagnation point flow over a shrinking sheet. *J. of Appl. Fluid Mech*. 6, (1), pp. 121-129.

[26] Makinde, O. D. (2012). Computational modeling of MHD unsteady flow and heat transfer toward a flat plate with Navier slip and Newtonian heating. Brazilian Journ. of Chem. Eng. 29, (2), pp. 159-166.

[27] Makinde, O. D., Charles, W. M. (2010). Computational dynamics of hydromagnetic stagnation flow towards a stretching sheet. *Appl. Comput. Math.* 9 (2), pp 243 – 251.

[28] Makinde, O. D., Mahabaleswar, U. S., Maheshkumar, N. (2013). Non-perturbative solution for hydromagnetic flow over a linearly stretching sheet. *Int. J. of Appl. Mech. & Eng.* 18, (3), pp. 935-943.

[29] Makinde, O. D. and Olanrewaju, P. O (2011). Unsteady mixed convection with Soret and Dufour effects past a porous plate moving through a Binary Mixture of Chemically reaction fluid, *Chemical Eng. Communications*. 198 (7), 920-938.

[30] Makinde, O. D. and Olanrewaju, P. O. (2012). Combined effects of internal heat generation and buoyancy force on boundary layer flow over a vertical plate with convective boundary condition. *Canadian J. of Chemical Eng*. 90, pp. 1289-1294.

[31] Makinde, O. D., Olanrewaju, P. O., Charles, W. M. (2011). Unsteady convection with Chemical reaction and radiative heat transfer past a flat porous plate moving through a binary mixture. *Afri. Mat.* 22 (1), pp. 65-78.

[32] Makinde, O. D. and Osalusi, E. (2006). MHD steady flow in a channel with slip at the permeable boundary. *Rom. Journ. Phys.* 51 (3-4), pp. 319-328.

[33] Manhata, P. K. (2013). Effects of variable viscosity and thermal conductivity on heat transfer over a stretching surface in the presence of uniform magnetic field. *World Academy of Science, Engineering and Technology*, 77, pp. 1059-1064.

[34] Moitsheki, R. J., Makinde, O. D. (2013). Computational modeling and similarity reduction of equations for transient fluid flow and heat transfer with variable properties, *Advances in Mechanical Eng*. ID 983962, pp. 1-8.

[35] Oahimire, J. I. and Olajuwon, B. I. (2013). Hydromagnetic flow near a stagnation point on a stretching sheet with variable thermal conductivity and heat source/sink. *Int. J. of Appl. Sc. Eng*. 11 (3), pp. 331-341.

[36] Olanrewaju, P. O. (2012). Effects of internal heat generation on hydromagnetic non-Darcy flow and heat transfer over a stretching sheet in the presence of thermal radiation and Ohmic dissipation. *World Applied Sciences Journ. (Special Issue of Appl. Math.),* 16, pp. 37-45.

[37] Olanrewaju, P. O. and Gbadeyan, J. A. (2011). Effects of Soret, Dufour, chemical reaction, thermal radiation and volumetric heat generation/absorption and a mixed convention stagnation point flow on an isothermal vertical plate in porous media. *The Pacific Journ. Sci.Tech. [PJST]*. 12 (2),pp. 234-245.

[38] Olanrewaju, P. O. and Adeniyan, A. (2013). Dufour and Soret effects on MHD free convection with thermal radiation and mass transfer past a vertical plate embedded in a porous medium, Nonlinear Sci. Lett. A. 4 (1), pp. 21-34.

[39] Olanrewaju, P. O. and Adesanya, A. O. (2011). Effects of radiation and viscous dissipation on stagnation flow of a micropolar fluid towards a vertical permeable surface, *Australian J. of Basic Appl. Sciences*, 5 (9), 2279-2289.

[40] Olanrewaju, P. O., Alao, F. I. and Adeniyan, A. (2013). Effects of thermal-diffusion, diffusion-thermo, magnetic field and viscous dissipation on unsteady mixed convection flow past a porous plate moving through a binary mixture of chemically reacting fluid, *Thermal Energy and Power (TEPE).* 2 (3), pp. 118-131.

[41] Rangi, R. R.and Ahmad, N. (2012). Boundary layer flow past a stretching cylinder and heat transfer with variable thermal conductivity. *Appl. Math.* 3, pp. 205-209.

[42] Seddeek, M. A. (2004). Thermal-diffusion and diffusion-thermo effects flow and heat transfer over an accelerating surface with heat source in the presence of suction and blowing in the case of variable viscosity. *Acta Mechanica,* 177 (1-2), pp. 83-94.

[43] Shrama, P. R and Singh, G. (2010). Steady MHD natural convection flow with variable electrical conductivity and heat generation along an isothermal vertical plate. *Tamkang Journ. of Sci. and Eng*. 13 (3), pp. 235-242.

[44] Singh, G. and Makinde, O. D. (2013). MHD slip flow of viscous fluid over an isothermal reactive stretching sheet. *Annals Faculty Eng. Hunedoara-Int. Journ. of Engineering.* 11 (2), pp. 41-46.

[45] Wong, S. W., Awang, M. A. O., Ishak, A. (2013). Stagnation point flow towards a vertical, nonlinearly stretching sheet with heat flux, *J. of . Appl. Mat*. Article ID:528717, pp. 1-7.

[46] Yian, L. Y., Ishak, A. and Pop, I. (2011). MHD stagnation point flow with suction towards a shrinking sheet. *Sains Malasiana*. 40 (10), pp. 1179-1186.

ADETUNJI ADENIYAN, DEPARTMENT OF MATHEMATICS, UNIVERSITY OF LAGOS, LAGOS, NIGERIA